

Ti influence on the electrochemical performance of $\text{Li}_3\text{V}_2(\text{PO}_4)_3$ cathode materials synthesized by a sol-gel method

You Wang*

College of Materials and Chemical Engineering, Hezhou University, Hezhou 542899, China
351569714@qq.com

*Corresponding author

Abstract: $\text{Li}_3\text{V}_2(\text{PO}_4)_3/\text{C}$ and $\text{Li}_3\text{V}_{2-x}\text{Ti}_x(\text{PO}_4)_3/\text{C}$ ($x=0.03, 0.05, 0.07$) cathode materials are synthesized by a solid-state method and a sol-gel method, respectively. X-ray diffraction (XRD) and scanning electronic microscopic (SEM) are employed to characterize the structures and morphologies of the as-prepared samples. The XRD patterns show that Ti-doping does not alter the monoclinic structure of $\text{Li}_3\text{V}_2(\text{PO}_4)_3$ and does not create a new phase as well. The SEM images show that Ti-doping can prevent the aggregations of the fine grains compared with the pure $\text{Li}_3\text{V}_2(\text{PO}_4)_3/\text{C}$. The electrochemical measurements show that Ti doping can improve the cycling and rate performance of LVP/C composite. The improved electrochemical properties of the $\text{Li}_3\text{V}_{2-x}\text{Ti}_x(\text{PO}_4)_3/\text{C}$ cathode materials may be attributed to the enhanced ionic and electronic conductivities caused by Ti doping.

Keywords: Lithium-ion batteries; cathode material; $\text{Li}_3\text{V}_2(\text{PO}_4)_3/\text{C}$; Ti-doping; sol-gel method

1. Introduction

Over decades lithium-ion batteries have achieved revolutionary progress and have been world-widely used as the power sources of electric vehicles (EV), hybrid electric vehicles (HEV), mobile phones, laptops, smart grids, etc. The emergence of olive-type cathode material LiFePO_4 (LFP) [1] has attracted extensive attention because of its excellent electrochemical performance and economical value. Based on a long-run research, nowadays, it has been successfully used in EV and HEV by BYD. Compared to LFP, monoclinic $\text{Li}_3\text{V}_2(\text{PO}_4)_3$ (LVP) exists a larger space housing lithium ions formed by sharing oxygen vertexes with tortuous VO_6 octahedral and PO_4 tetrahedral, which allows lithium-ions to migrate faster in the channels [2,3]. In particular, when charging from 3.0V to 4.8V LVP can reversibly extract three Li^+ ions, corresponding to a capacity of 197mAh g^{-1} , which is much higher than that of LFP. In addition, its preferable intercalation potential, thermal stability and rate performance also give LVP a chance to be a promising alternative cathode material. However, two dominant defects of low ion conductivity and poor electronic conductivity seriously limit its commercial applications [2,4]. To solve these problems, recent years, lots of efforts have been made by researchers including carbon coating [5-9], alien metal ions doping [10-19] and nanotailoring [20-22], etc.

In fact, each route applied to modify LVP is associated with carbon coating, which demonstrates that pure metal ionic doping will finally fail to improve the electrochemical performances of LVP. Traditionally, the dopants and carbon sources need to be added separately, which increases the steps and costs. Therefore, searching for such transition metal organic compounds that can be used as both cation and carbon sources becomes much sensible. Titanate coupling agent TC-Wt (TCA-TW) is the very one we want to find because it contains both titanium and carbon elements and usually acts as dispersant and bonding agent which can easily coat on the surface of LVP precursors. Upon the above considerations, TCA-TW may be an intriguing modifier for LVP. On the other hand, there have been few reports about its application in LVP modification so far. Thus, in the previous work [23], we reported the $\text{Li}_3\text{V}_{2-x}\text{Ti}_x(\text{PO}_4)_3/\text{C}$ composites synthesized by a solid state method using TCA-TW as modifier. And the modified samples all exhibited remarkably enhanced electrochemical properties owing to the combination of carbon coating and Ti^{4+} doping.

However, some defects still exist for a solid state method, such as producing large and uneven particles, requiring high calcining temperature, and so on. Comparatively, for a sol-gel method, the materials can be mixed in molecular level, which is favorable for preparing fine and even grains and

can reduce the calcining temperature. Here, we demonstrate a sol-gel route for modifying LVP by TCA-TW. In order to compare with the solid state route, the structure and electrochemical properties of the modified samples were investigated.

2. Experimental

The $\text{Li}_3\text{V}_2(\text{PO}_4)_3/\text{C}$ sample was prepared upon the procedure introduced in [23]. $\text{Li}_3\text{V}_{2-x}\text{Ti}_x(\text{PO}_4)_3/\text{C}$ ($x=0.03, 0.05, 0.07$) composites were prepared by a sol-gel method using $\text{LiOH} \cdot \text{H}_2\text{O}$ (A.R.), V_2O_5 (A.R.), $\text{NH}_4\text{H}_2\text{PO}_4$ (A.R.), H_2O_2 (30 wt. %) and TCA-TW as starting materials. Specially, TCA-TW served as dispersant, chelating agent, carbon and titanium sources during the process. Firstly, needed V_2O_5 was dissolved in moderate H_2O_2 by magnetically stirring until a clear orange solution was formed. Subsequently, stoichiometric amount of TCA-TW, $\text{LiOH} \cdot \text{H}_2\text{O}$, $\text{NH}_4\text{H}_2\text{PO}_4$ were added successively. Finally, the above mentioned solution was stirred vigorously at 85°C until a blue gel was formed. After dried at 80°C for 24h in vacuum, the obtained precursor was sent into a tube furnace and sintered at 350°C for 3h under an argon flow with a heating rate of $5^\circ\text{C}/\text{min}$ to drive away NH_3 and water. Then elevated the temperature to 700°C with the same heating rate and sintered the precursor for another 12h to obtain the $\text{Li}_3\text{V}_{2-x}\text{Ti}_x(\text{PO}_4)_3/\text{C}$ samples.

The crystalline structures of the as-prepared samples were measured via X-ray diffraction (XRD, XPert-Pro) using $\text{Cu K}\alpha$ radiation scanning in the range of 10° to 80° (2θ), with a step size of 0.02° . The morphologies of the samples were characterized by a field-emission scanning electron microscope (Philips, FEI Quanta 200FEG).

The electrochemical characterizations were performed using a CR2025 coin-type cell. First, 10wt. % acetylene black, 10 wt. % polyvinylidene fluoride (PVDF) binder and 80wt. % active material were mixed and then dispersed in N-methylpyrrolidone to get a slurry. Second, the blended slurry was pasted onto an aluminum current collector and dried at 100°C for 12h in vacuum. Then the cells were assembled in an argon-filled glove box with $\text{Li}_3\text{V}_{2-x}\text{Ti}_x(\text{PO}_4)_3/\text{C}$ as the cathode, Li metal as the anode and 1M LiPF_6 solution in a mixture of ethylene carbonate and dimethyl carbonate with a volumetric ratio of 1:1 as the electrolyte. The cells were charged and discharged in the voltage range of 3.0-4.2V at room temperature. Cyclic voltammograms (CV) and electrochemical impedance spectroscopy (EIS) tests were performed with a CHI860D electrochemical work station. The CV curves for the above test cells were recorded in a potential range of 3.0-4.5V at a scanning rate of 0.1mV/s. EIS experiments were carried out with the frequency ranging from 10kHz to 10mHz.

3. Results and discussion

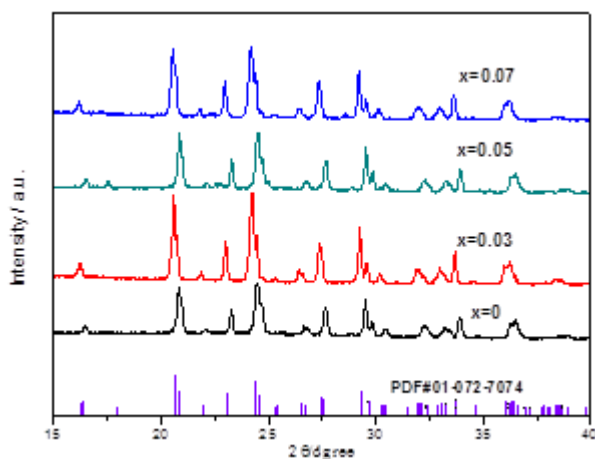
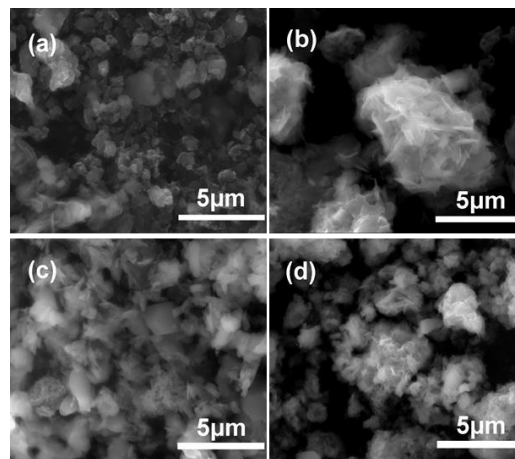


Figure 1: XRD patterns of $\text{Li}_3\text{V}_{2-x}\text{Ti}_x(\text{PO}_4)_3/\text{C}$ samples

Fig.1 shows the XRD patterns of $\text{Li}_3\text{V}_{2-x}\text{Ti}_x(\text{PO}_4)_3/\text{C}$ ($x=0, 0.03, 0.05, 0.07$) samples. It demonstrates that all the samples are well consistent with PDF#01-072-7074 which presents monoclinic $\text{Li}_3\text{V}_2(\text{PO}_4)_3$ (space group $\text{P}2_1\text{n}$), indicating that Ti doping does not alter the structure of LVP. No impurity phase are detected, implying that Ti ions have been inserted into the LVP crystal lattice [11, 12]. However, a slightly shift of the peaks position can be observed as a result of Ti doping,

which may be associated with the changes of the lattice parameters [19,24]. On the other hand, the absence of carbon peaks in the patterns proves the residue carbon is amorphous.

Fig.2 shows the SEM images of $\text{Li}_3\text{V}_{2-x}\text{Ti}_x(\text{PO}_4)_3/\text{C}$ samples. Fig.2 (a) presents the microstructure of pure LVP/C sample synthesized by a solid state route, in which a wide-scale aggregation of fine grains of about $1\mu\text{m}$ can be observed. It indicates a poor electrochemical performance due to the diffusion paths for lithium ions are lengthened. Fig.2 (b)-(d) exhibit the microstructure of the modified samples with $x=0.03, 0.05, 0.07$, respectively. When $x=0.05$, the sample shows the best image consists of uniform and relative regular particles with an average size of $1\sim 2\mu\text{m}$, which may play a favorable role in improving the electrochemical performances of LVP by reducing the diffusion distance of lithium ions. Moreover, the carbon decomposed from TCA-TW closely connects the LVP particles like a net, which can facilitate the electronic transfer among the particles. On the contrary, when $x=0.03$ or 0.05 , the small particles aggregate together to form the larger secondary particles, which is unfavorable to the migration of lithium ions and electronics in the bulk crystals.



(a) $x=0$; (b) $x=0.03$; (c) $x=0.05$; (d) $x=0.07$

Figure 2: SEM images of $\text{Li}_3\text{V}_{2-x}\text{Ti}_x(\text{PO}_4)_3/\text{C}$ samples

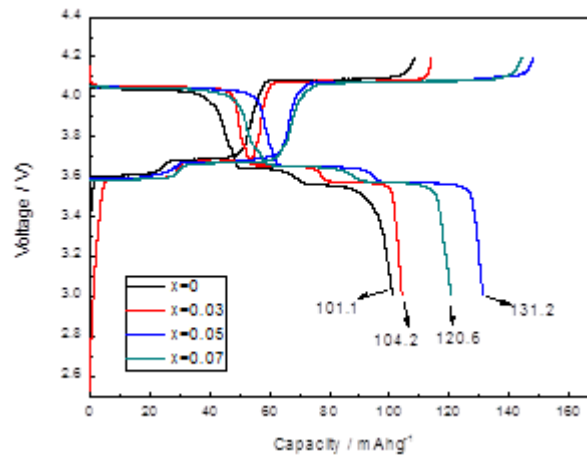


Figure 3: Initial charge-discharge curves of $\text{Li}_3\text{V}_{2-x}\text{Ti}_x(\text{PO}_4)_3/\text{C}$ at 0.1C rate

Fig.3 shows the initial charge-discharge curves of $\text{Li}_3\text{V}_{2-x}\text{Ti}_x(\text{PO}_4)_3/\text{C}$ samples at 0.1C (14mA/g) in the potential range of 3.0-4.2V. Regardless of Ti content(x), for the charge curves, three plateaus at 3.59, 3.68 and 4.08V are observed, which correspond to the extraction of lithium ions and the phase transition of $\text{Li}_x\text{V}_2(\text{PO}_4)_3$ from $x=3.0$ to 2.5, 2.0 and 1.0, respectively. The first lithium ion is extracted in two steps(3.59 and 3.68V) because of the existence of an ordered phase $\text{Li}_{2.5}\text{V}_2(\text{PO}_4)_3$ at a mixed $\text{V}^{3+}/\text{V}^{4+}$. Then, a single step removal of the second lithium ion at 4.08V can be observed, which corresponds to the complete oxidation of V^{3+} to V^{4+} . Three corresponding plateaus at 4.04, 3.66 and 3.55V are observed in the discharge curves, corresponding to the reinsertion of two lithium ions accompanied with the phase transition of $\text{Li}_x\text{V}_2(\text{PO}_4)_3$ from $x=1.0$ to 1.5, 2.0 and 3.0[21]. Another aspect, the charge plateaus of LVP/C are higher than those of the modified ones and the discharge plateaus are lower than the later, indicating that the ionic and electronic conductivities of the pure

sample are poorer than the doped ones, which is well consistent with the morphological analysis in Fig.2. As shown, the initial charge specific capacities of $\text{Li}_3\text{V}_{2-x}\text{Ti}_x(\text{PO}_4)_3/\text{C}$ with $x=0, 0.03, 0.05$ and 0.07 are 108.6, 114.0, 147.8 and 144.4 mAh g^{-1} , respectively, and the initial discharge capacities are 101.1, 104.2, 131.2 and 120.6 mAh g^{-1} , respectively. The corresponding coulombic efficiencies are 93.1%, 91.4%, 88.8% and 83.5%, respectively. The above results reveal that Ti content has great influence on the charge-discharge performance of $\text{Li}_3\text{V}_{2-x}\text{Ti}_x(\text{PO}_4)_3/\text{C}$ samples, which may be associated with the changes of the microstructures of LVP triggered by Ti doping. And the enhanced electrochemical performances of Ti-doped LVP can be ascribed to the improved ionic and electronic conductivities [23].

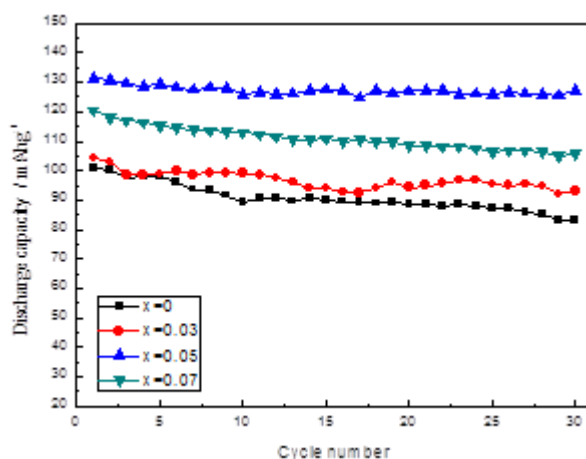


Figure 4: Cycling performance of $\text{Li}_3\text{V}_{2-x}\text{Ti}_x(\text{PO}_4)_3/\text{C}$ at 0.1C rate

Fig.4 shows the cycling performance curves of $\text{Li}_3\text{V}_{2-x}\text{Ti}_x(\text{PO}_4)_3/\text{C}$ at 0.1C rate in the potential range of 3.0-4.2V. As shown that the initial discharge capacities at 0.1C rate are 101.1, 104.2, 131.2 and 120.6 mAh g^{-1} , respectively, when $x=0, 0.03, 0.05$ and 0.07 . The corresponding discharge capacities are 83.1, 93.2, 127.3 and 105.9 mAh g^{-1} , respectively, after 30 cycles. The retention rates of capacity keep at 82.2%, 89.4%, 97.0% and 87.8%, respectively. The results indicate that the cycling capability of the LVP can be improved by Ti doping and the Ti content also affects the effect of doping. The improved cycling capability of LVP should be ascribed to the ionic and electronic conductivities, which has been discussed in the charge-discharge performances.

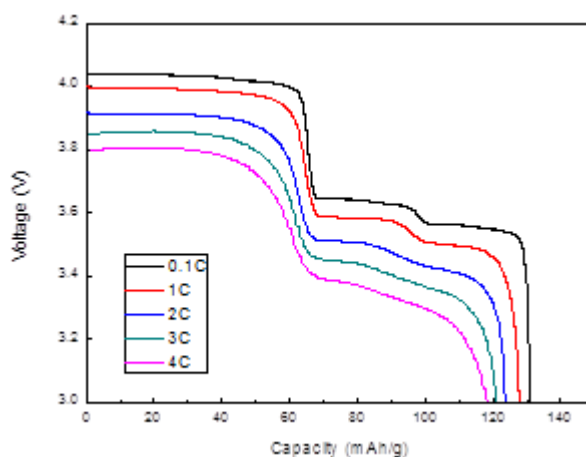


Figure 5: Rate performance of $\text{Li}_3\text{V}_{1.95}\text{Ti}_{0.05}(\text{PO}_4)_3/\text{C}$ sample

The rate performance is usually used to characterize the ionic conductivity of LVP cathode materials. To investigate the influence of Ti on the rate performance of LVP/C composite, the cell fabricated from $\text{Li}_3\text{V}_{1.95}\text{Ti}_{0.05}(\text{PO}_4)_3/\text{C}$ composite was charged and discharged at 0.1C for two cycles in the potential range of 3.0-4.2V. Then, the charge rate was fixed at 1C and the discharge rates were changed from 1C to 2C, 3C and 4C, respectively. As shown in Fig.5, the discharge capacities slightly decreases from 131.2 to 127.7, 123.6, 121 and 118.2 mAh g^{-1} , respectively, as the discharge rate increases from 0.1C to 1C, 2C, 3C and 4C, respectively, which illustrates that a preferable rate

performance can be accessed by incorporating 5% Ti into LVP/C composite and verifies that Ti incorporation should be responsible for the enhancement of the ionic conductivity of LVP/C composite.

The reversibility of the electrochemical reaction for $\text{Li}_3\text{V}_{1.95}\text{Ti}_{0.05}(\text{PO}_4)_3/\text{C}$ composite and LVP/C composite are identified by CV tests as shown in Fig.6. Three oxidation peaks at 3.65V, 3.72V and 4.13V and corresponding reduction peaks at 3.52V, 3.61V and 3.98V are observed for $\text{Li}_3\text{V}_{1.95}\text{Ti}_{0.05}(\text{PO}_4)_3/\text{C}$ composite, which is well agree with the charge-discharge curve shown in Fig.2. For LVP/C composite, the oxidation peaks appear at 3.67V, 3.74V and 4.14V, respectively, with corresponding reduction peaks at 3.53V, 3.60V and 4.14V, respectively. The positions of the oxidation peaks shift to the right and those of the reduction peaks shift to the left compared to the former, which indicates that the electrochemical resistance of LVP/C is larger than that of $\text{Li}_3\text{V}_{1.95}\text{Ti}_{0.05}(\text{PO}_4)_3/\text{C}$ composite. This conclusion can be confirmed in Fig.7. The CV plots in Fig.6 clearly demonstrate that the electrochemical reversibility of LVP/C composite can be improved by Ti doping.

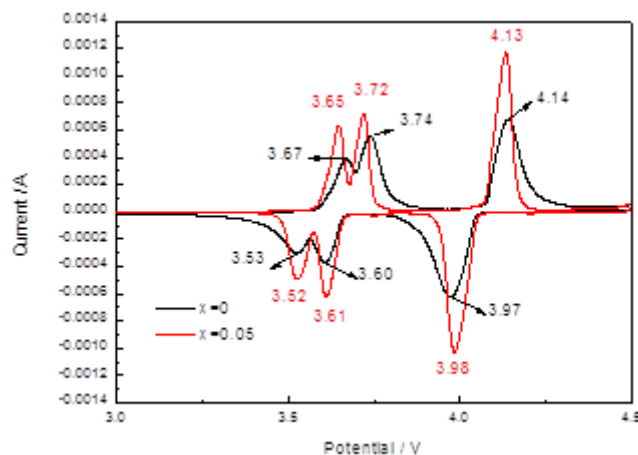


Figure 6: CV curves of $\text{Li}_3\text{V}_2(\text{PO}_4)_3/\text{C}$ and $\text{Li}_3\text{V}_{1.95}\text{Ti}_{0.05}(\text{PO}_4)_3/\text{C}$ in the potential range of 3.0-4.5V at 0.1mV s^{-1} scan rate

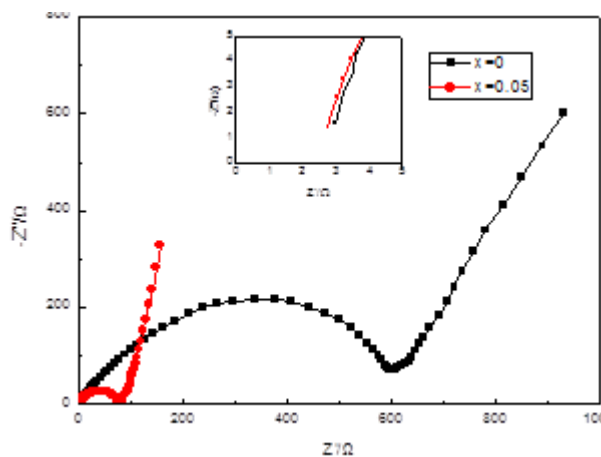


Figure 7: Nyquist plots of $\text{Li}_3\text{V}_2(\text{PO}_4)_3/\text{C}$ and $\text{Li}_3\text{V}_{1.95}\text{Ti}_{0.05}(\text{PO}_4)_3/\text{C}$

The excellent kinetic property of $\text{Li}_3\text{V}_{1.95}\text{Ti}_{0.05}(\text{PO}_4)_3/\text{C}$ composite can be further understood by EIS analysis showing all sorts of resistance linked to charge transfer at electrode/electrolyte interface or inside electrode. The Nyquist plots of $\text{Li}_3\text{V}_2(\text{PO}_4)_3/\text{C}$ and $\text{Li}_3\text{V}_{1.95}\text{Ti}_{0.05}(\text{PO}_4)_3/\text{C}$ are shown in Fig.7. The cells were charged and discharged for 4 times at 0.1C before the EIS tests. It is clear that each plot is comprised of a depressed semicircle in high frequency region and a straight line in low frequency region. The intercept at real axis in the very high frequency is related to the solution resistance (R_s). The diameter of the semicircle presents the charge transfer resistance (R_{ct}). The inclined line in low frequency corresponds to the Warburg impedance, which represents the diffusion of lithium ions in the cathode material. As shown, the R_s values of both samples are very similar, but the R_{ct} value of $\text{Li}_3\text{V}_{1.95}\text{Ti}_{0.05}(\text{PO}_4)_3/\text{C}$ composite is much smaller than that of LVP/C composite, which indicates that the transportation of lithium ions and electronics through the electrode/electrolyte interface becomes

easier by Ti doping. The reason why $\text{Li}_3\text{V}_{1.95}\text{Ti}_{0.05}(\text{PO}_4)_3/\text{C}$ composite has a lower R_{ct} value may be ascribed to its improved microstructure and surface by Ti doping.

4. Conclusions

$\text{Li}_3\text{V}_{2-x}\text{Ti}_x(\text{PO}_4)_3/\text{C}$ ($x=0, 0.03, 0.05, 0.07$) cathode materials have been successfully synthesized by a sol-gel method. It is found that Ti doping does not change the crystal structure of LVP. But it is favorable for the formation of well-dispersed fine particles connected by amorphous carbon. With respect to LVP/C, $\text{Li}_3\text{V}_{1.95}\text{Ti}_{0.05}(\text{PO}_4)_3/\text{C}$ exhibits excellent cycling and rate performances, which is associated with the enhanced ionic and electronic conductivity by Ti doping.

References

- [1] A.K.Padhi, K.S.Nanjundaswamy, J.B.Goodenough. Phosphate-olives as positive-electrode materials for rechargeable lithium batteries. *J. Electrochem. Soc.* 1997, 144: 1188-1194.
- [2] X.H.Rui, N.Ding, J.Liu, C.Li, C.H.Chen. Analysis of the chemical diffusion coefficient of lithium ions in $\text{Li}_3\text{V}_2(\text{PO}_4)_3$ cathode material [J]. *Electrochimica Acta*, 2010, 55: 2384-2390.
- [3] S.C.Yin, H.Grondey, P.Strobel, M. Anne, L.F. Nazar. Electrochemical property: structure relationships in monoclinic $\text{Li}_{3-y}\text{V}_2(\text{PO}_4)_3$ [J]. *J. Am. Chem. Soc.*, 2003, 125: 10402- 10411.
- [4] S.C. Yin, P.S. Strobel, H.Grondey, L.F.Nazar. $\text{Li}_2.5\text{V}_2(\text{PO}_4)_3$: A room-temperature analogue to the fast-ion conducting high-temperature γ -phase of $\text{Li}_3\text{V}_2(\text{PO}_4)_3$ [J]. *Chem. Mater.*, 2004, 16: 1456-1465.
- [5] M.M.Ren, Z.Zhou, X.P.Gao, W.X.Peng, J.P.Wei. Core-Shell $\text{Li}_3\text{V}_2(\text{PO}_4)_3/\text{C}$ composites as cathode materials for lithium-ion batteries [J]. *J. Phys. Chem. C*, 2008, 112: 5689-5693.
- [6] C.Sun, S.Rajasekhara, Y.Dong, J.B.Goodenough. Hydrothermal synthesis and electrochemical properties of $\text{Li}_3\text{V}_2(\text{PO}_4)_3/\text{C}$ -based composites for lithium-ion batteries [J]. *ACS Appl. Mater. Interfaces*, 2011, 3 : 3772-3776.
- [7] Z.H.Yuan, J.Ma, X.Chen, K.Y.Liu. P123-Assisted rheological phase reaction synthesis and electrochemical performance of $\text{Li}_3\text{V}_2(\text{PO}_4)_3/\text{C}$ cathode [J]. *Acta Phys.-Chim. Sin.* 2012, 28: 2898-2904.
- [8] C.Deng, S.Zhang, Z.Dong, et al. Effects of carbon coating on the structure, morphology and electrochemical performance of $\text{Li}_3\text{V}_2(\text{PO}_4)_3$ cathode material prepared by solid state method [J]. *Int. J. Electrochem. Sci.*, 2012, 7: 6951-6958.
- [9] R.Y.Zhang, Y.Q.Zhang, K.Zhu, F.Du, Q.Fu, X.Yang, Y.H.Wang, X.F.Bie, G.Chen, Y.J.Wei. Carbon and RuO_2 binary surface coating for the $\text{Li}_3\text{V}_2(\text{PO}_4)_3$ cathode material for lithium-ion batteries [J]. *ACS Appl. Mater. Interfaces*, 2014, 6 : 12523-12530.
- [10] J.Barker, R.K.B.Gover, P.Burns, A.Bryan. The effect of Al substitution on the electrochemical insertion properties of the lithium vanadium phosphate, $\text{Li}_3\text{V}_2(\text{PO}_4)_3$ [J]. *J. Electrochem. Soc.*, 2007, 154: 307-313.
- [11] S.K.Zhong, L.T.Liu, J.Q.Jiang, et al. Preparation and electrochemical properties of Y-doped $\text{Li}_3\text{V}_2(\text{PO}_4)_3$ cathode materials for lithium batteries [J]. *J. Rare Earths*, 2009, 27 : 134-137.
- [12] S.K. Zhong, B. Zhao, Y.W. Li, et al. Synthesis and electrochemical properties of Cr-doped $\text{Li}_3\text{V}_2(\text{PO}_4)_3$ cathode materials for lithium-ion batteries [J]. *Journal of Wuhan University of Technology-Mater. Sci. Ed.*, 2009, 24: 343-346.
- [13] J.Zhai, M.S.Zhao, D.D.Wang. Effect of Mn-doping on performance of $\text{Li}_3\text{V}_2(\text{PO}_4)_3/\text{C}$ cathode material for lithium ion batteries [J]. *Trans. Nonferrous Met. Soc. China*, 2011, 21: 523-528.
- [14] D.J.Ai, K.Y.Liu, Z.G.Lu, et al. Aluminothermal synthesis and characterization of $\text{Li}_3\text{V}_{2-x}\text{Al}_x(\text{PO}_4)_3$ cathode materials for Lithium ion batteries [J]. *Electrochem Acta*, 2011, 56: 2823-2827.
- [15] Y.Xia, W.K.Zhang, H.Huang, et al. Synthesis and electrochemical properties of Nb-doped $\text{Li}_3\text{V}_2(\text{PO}_4)_3/\text{C}$ cathode materials for lithium-ion batteries [J]. *Materials Science and Engineering B*, 2011, 176: 633-639.
- [16] J.S.Huang, L.Yang, K.Y.Liu, et al. Synthesis and characterization of $\text{Li}_3\text{V}_{2-2x/3}\text{Mg}_x(\text{PO}_4)_3/\text{C}$ cathode material for Lithium-ion batteries [J]. *J Power Sources*, 2010, 195: 5013-5018.
- [17] W.I.Wu, J.liang, J.Yan, W.F.Mao. Synthesis of $\text{Li}_3\text{Ni}_x\text{V}_{2-x}(\text{PO}_4)_3/\text{C}$ cathode materials and their electrochemical performance for lithium ion batteries [J]. *J. Solid State Electrochem* 2013, 17: 2027-2033.
- [18] C.X. Ma, W.F. Mao, Z.Y.Tang, Q. Xu. Synthesis of $\text{Li}_3\text{W}_x\text{V}_{2-x}(\text{PO}_4)_3/\text{C}$ cathode materials and their electrochemical performance for lithium-ion batteries [J]. *J. Solid State Electrochem.*, 2015, 19: 519-524.
- [19] D.W.Han, S.J.Lim, Y-II.Kim, S.H.Kang, Y.C.Lee, Y.M.Kang. Facile lithium ion transport through super ionic pathways formed on the surface of $\text{Li}_3\text{V}_2(\text{PO}_4)_3/\text{C}$ for high power Li ion battery [J]. *Chem. Mater.* 2014, 26: 3644-3650.

- [20] A.Q.Pan, D.W.Chio, J.G.Zhang, S.Q.Liang, G.Z.Cao, Z.M.Nie, B.W.Arey, J.Liu. High-rate cathodes based on $\text{Li}_3\text{V}_2(\text{PO}_4)_3$ nanobelts prepared via surfactant-assisted fabrication[J]. *J.Power. Sources*, 2011, 196: 3646-3649.
- [21] A.Q.Pan, J.Liu, J.G.Zhang, W.Xu, G.Z.Cao, Z.M.Nie, B.W.Arey, S.Q.Liang. Nano-structured $\text{Li}_3\text{V}_2(\text{PO}_4)_3$ /carbon composite for high-rate lithium-ion batteries [J]. *Electrochem. Commun*, 2010, 12: 1674-1677.
- [22] Q.L.Wei, Q.Y.An, D.D.Chen, L.Q.Mai, S.Y.Chen, Y.L.Zhao, K.M.Hercule, L.Xu, M. Minhas-Khan, Q.J. Zhang. One-Pot synthesized bicontinuous hierarchical $\text{Li}_3\text{V}_2(\text{PO}_4)_3/\text{C}$ mesoporous nanowires for high-rate and ultralong-life lithium-ion batteries[J]. *Nano Lett.*, 2014, 14: 1042-1048.
- [23] S.K.Zhong, Y.Wang, L.Wu, J.Q.Liu. Synthesis and electrochemical properties of Ti-doped $\text{Li}_3\text{V}_2(\text{PO}_4)_3/\text{C}$ cathode materials [J]. *Rare Met.*, 2015, 34: 586-589.
- [24] S.C.Liu, S.C.Li, K.L.Huang, C.H.Chen. Effect of doping Ti^{4+} on the structure and performances of $\text{Li}_3\text{V}_2(\text{PO}_4)_3$ [J]. *Acta Phys. -Chim. Sin.*, 2007, 23: 537- 542.